IL01

Molecular Contrast Mechanisms in Higher Harmonic Generation Microscopy

Chi-Kuang Sun[1,2]

[1]*Department of Electrical Engineering and Graduate Institute of Photonics and Optoelectronics, National Taiwan University, Taipei, Taiwan*

[2]*Research Center for Applied Sciences, Academia Sinica, Taipei, Taiwan*

Correspondence e-mail address: sun@cc.ee.ntu.edu.tw

In this presentation, we will review the physics and recent applications of the least-invasive in vivo optical harmonic microscopy,[1] with a focus on the molecular contrast mechanism. Optical higher harmonic-generations, including second harmonic generation (SHG) and third harmonic generation (THG), leave no energy deposition to the interacted matters due to their energy-conservation characteristic, providing the "noninvasiveness" nature desirable for biological studies. Combined with their nonlinearity, harmonic generation microscopy provides three-dimensional (3D) sectioning capability, offering new insights into live samples. By choosing the lasers working in the high penetration window, we have developed a noninvasive *in vivo* light microscopy with submicron 3D resolution and high penetration, utilizing endogenous higher-harmonic-generation signals in live specimens. THG contrast was found to be contributed from lipid,[1] oxy-hemoglobin, elastin fibers,[2] and laminated organelles. SHG contrast was found to be contributed from skeleton muscle,[3,4] cardiac muscle, collagen fibrils,[3] axons,[1] mitosis spindles,[1] zona pellucida, strain in enamel, and polyhedral inclusion bodies[5] of nuclear polyhedrosis viruses. From a biophysics point of view, we will discuss the origins of these signals through spatial anisotropy,[3,4,5] Gouy phase shift effect,[1] and multiphoton-resonance of the harmonic generations.[2]

(1) C.-K. Sun, et al., "Higher harmonic generation microscopy for developmental biology," *Journal of Structural Biology* 147 (1), 19-30 (2004).

(2) C.-H. Yu, et al., "*In vivo* and *ex vivo* imaging of intra-tissue elastic fibers using third-harmonic-generation microscopy," *Optics Express* 15 (18), 11167-11177 (2007).

(3) S.-W. Chu, et al., "Nonlinear bio-photonic crystal effects revealed with multimodal nonlinear microscopy," *Journal of Microscopy-Oxford* 208 (3), 190-200 (2002).

(4) S.-W. Chu, et al, "Studies of $\chi^{(2)}/\chi^{(3)}$ tensors in submicron-scaled bio-tissues by polarization harmonics optical microscopy," *Biophysical Journal* 86 (6), pp. 3914-3922 (2004).

(5) T.-M. Liu, et al., "Imaging polyhedral inclusion bodies of nuclear polyhedrosis viruses with second harmonic generation microscopy," to be published in *Optics Express* (2008).

IL02

Particle Movements and Membrane Deformations on a Living Cell Characterized by Optical Tracking and Widefield Profilometry

Chau-Hwang Lee

Research Center for Applied Sciences, Academia Sinica, Taipei 11529, Taiwan

Correspondence e-mail address: clee@gate.sinica.edu.tw

We directly observe the internalization of gold nanoparticles on the membrane of a living cell by using non-interferometric widefield optical profilometry (NIWOP) (1,2). NIWOP traces the height of an 80-nm gold particle on the membrane by calibrating the change of light intensity scattered from the particle. Comparing the heights of the nanoparticle and those of nearby membranes, we identify the occurrence of particle internalization. Combining fluorescence microscopy with NIWOP, we also find actin aggregation around the site of the internalization process (as shown in Fig. 1), which is an indication of endocytosis (3).

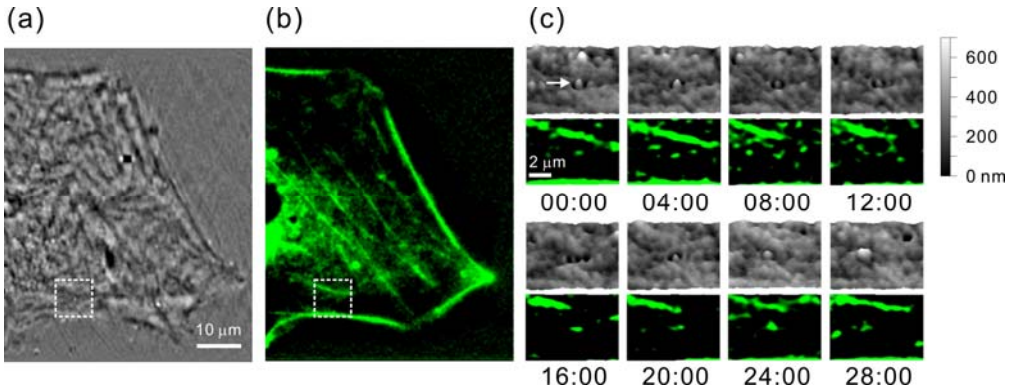

Figure. (a) Membrane topography of a fibroblast obtained by NIWOP. (b) GFP–actin distribution of the same cell in (a). (c) Time-lapse images of the region enclosed by the dashed squares in (a) and (b). Timing format, min:sec. (4)

In addition to the particle motion driven by intracellular proteins, we also measured the membrane deformations under the modulation of localized piconewton magnetic force produced by a sub-micrometer magnetic needle (5). The magnetic force was applied to fibronectin-coated paramagnetic beads that bound to transmembrane protein integrins. We elucidated the correlation between the bead moving speed and membrane deformations. According to the moving directions of the paramagnetic beads, a model based on the mediation by actin cytoskeletons is proposed to explain the observation results (6).

(1) Wang, C.-C., J.-Y. Lin, and C.-H. Lee. 2005. *Opt. Express* 13:10665–10672.
(2) Wang, C.-C., J.-Y. Lin, H.-C. Chen, and C.-H. Lee. 2006. *Opt. Lett*. 31:2873–2875.
(3) Merrifield, C. J. 2004. *Trends Cell Biol*. 14:352–358.
(4) Wang, C.-C., J.-Y. Lin, C.-W. Lee, C.-Y. Huang, P.-K. Wei, and C.-H. Lee. 2008. Internalization of nanoparticles on cell membranes observed by non-interferometric widefield optical profilometry. *Appl. Opt.* in press.
(5) Matthews, B. D., D. A. LaVan, D. R. Overby, J. Karavitis, and D. E. Ingber. 2004. *Appl. Phys. Lett.* 85:2968–2970.
(6) Wang, C.-C., H.-J. Jian, C.-W. Wu, and C.-H. Lee. 2008. Cell membrane deformations under magnetic force modulation characterized by optical tracking and profilometry. *Microsc. Res. Tech*. in press.

IL03

Intravital Multiphoton Hepatic Microscopy – a New Approach for Understanding Liver

Chen-Yuan Dong[1], Hsuan-Shu Lee[2,3]

[1]*Department of Physics, National Taiwan University*

[2]*Institute of Biotechnology, College of Bio-Resources and Agriculture, National Taiwan University*

[3]*Department of Internal Medicine, National Taiwan University Hospital*

Correspondence e-mail addresses: C. Y. Dong at cydong@phys.ntu.edu.tw or H. S. Lee at benlee@ntu.edu.tw

As in many areas of biomedical sciences, hepatology has depended heavily on histological procedures for pathological diagnosis and indirect biochemical assays such as the measurement of albumin and transaminase contents for inferring hepatic functions. However, the sample fixation procedures associated with histological examination prevent dynamic physiological processes to be studied. Furthermore, indirect biochemical assays do not represent a direct evaluation of organ function. In this work, we extend intravital multiphoton microscopy for the *in vivo* investigation of hepatic processes. Through the installation of intravital hepatic imaging chambers (IHIC), dynamic physiological processes such as metabolite processing, bileduct ligation, effect of toxins on hepatocyte viability, and the effects of lipopolysaccharides can be investigated to unprecedented temporal and spatial resolution. In this presentation, I will describe this novel approach and demonstrate the aforementioned examples of hepatic physiological processes. We hope to develop this approach into an important methodology for revealing fundamental working dynamics of liver.

IL04

Single Molecule Studies of DNA Brushes

Wen-Tau Juan[1, 2], and Steven Chu[2]

[1]*Institute of Physics, Academia Sinica, Taipei, Taiwan*

[2]*Physics Department, Stanford University, Stanford, CA*

Correspondence e-mail address: wtjuan@phys.sinica.edu.tw

High density DNA brushes are constructed through end-tethering DNA molecules on a quartz substrate. At high grafting density, entropy driven DNA swelling of the brush layer with a parabolic monomer density distribution is observed. The conformation and the dynamics of individual end-tethered molecule inside the brush are studied using fluorescence microscopy. Our experimental data shows that, the brush bearing surface could be a protection layer for foreign objects and may have further biological implications.

IL05

Imaging small molecules with CARS microscopy

Wei Yuan Yang

Institute of Biological Chemistry, Academia Sinica, Taipei, Taiwan

Fluorescence microscopy possesses imaging capabilities at the single molecule level with high time resolutions. Despite the immense success of fluorescence based approaches, finding a suitable fluorescent label for one's molecule of interest (for fluorescence detection) is by no means always a trivial task. For example, fluorescent-labeling of small biomolecules oftentimes perturbs the molecules' native functions. Here we present Coherent anti-Stokes Raman Scattering (CARS) microscopy as a useful alternative for the imaging of small biomolecules.

IL06

Single Molecule Analysis Using Micro/Nanofluidic Devices

Chia-Fu Chou

Institute of Physics, Research Center for Applied Sciences, and Genomics Research Center, Academia Sinica, Taipei, Taiwan

Correspondence e-mail address: cfchou@phys.sinica.edu.tw

Fluidic Interfaces between micro- to nanoscale environments and the extreme confinement effects provided by nanofluidic channels have offered unique platforms to study single molecule behavior and new physics in these experimentally tailored fluidic environments. We will discuss three cases of using micro/nanofluidic devices for single molecule analysis: (1) molecular stretching in nanofluidic channels and its applications in direct mapping of transcriptional factors and single molecule DNA sequencing, (2) confinement-induced entropic recoiling of single DNA molecules at micro-nanofluidic interfaces, and (3) magnetic tweezers assisted study of metallic nanorod conjugated RecA-DNA interactions in microfluidic channels.

IL07

Activation Mechanism of Large-conductance Ca^{2+}-activated K^+ Channels by Intracellular Calcium: From Electrophysiological Facts to Structural Imagination

Chul-Seung Park

Department of Life Science, Gwangju Institute of Science and Technology (GIST)

Gwangju 500-712, Korea

Being activated independently by membrane depolarization and an increase in intracellular calcium, the large-conductance Ca^{2+}-activated K^+ (BK_{Ca}) channels play a key role in modulating a number of important physiological processes. While the membrane voltage is sensed by the membrane spanning regions, mainly the fourth transmembrane domain, the bulky cytoplasmic C-terminus is responsible for the calcium-dependent activation of the channel. Over the last few years, we have been interested in where the intracellular Ca^{2+} actually binds and how the binding of Ca^{2+} evokes the conformational change to open the channel pore. Using the known structure of procaryotic K^+ channels and bioinformatic tools, we were able to find key structural domains conserved in the cytosolic C-terminus of the mammalian BK_{Ca} channels. Molecular modeling and functional studies allowed us to envision the molecular mechanism of the channel activation by intracellular Ca^{2+}. The intracellular gating ring composed of hetero-octamer of RCK domains will be introduced as the sensor and transducer of intracellular Ca^{2+} for BK_{Ca} channel activation.

IL08

Cooperative K^+ Binding and Concerted K^+ transport in Inner Vestibule is Critical for Permeation in Kir2.1 Channel

Hsueh-Kai Chang[1], Laurence J. Marton[2], Kuo Kan Liang[3], and Ru-Chi Shieh[1*]

[1]*Institute of Biomedical Sciences, Academia Sinica, Taipei 11529, Taiwan*

[2]*Progen Pharmaceuticals, Inc., Redwood City, CA 94065, USA*

[3]*Division of Mechanics, Research Center for Applied Sciences, Academia Sinica, Taipei, 11529, Taiwan*

Correspondence e-mail address: ruchi@ibms.sinica.edu.tw

K^+ channels selectively allow K^+ ion conduction through their pores with high speed. K^+ ions are coordinated in the selectivity filter and concerted K^+ and water movements ensure high conductance. In channels with long pores, such as inward rectifier K^+ channels, many K^+ binding sites are located intracellular to the selectivity filter (inner vestibule), but the contribution of K^+ ions in this region to permeation is not well studied. The approach we used to investigating this area was to slow down the ion permeation process by blocking Kir2.1 channels with Ba^{2+} bound in the selectivity filter. We then observed the role K^+ ions in the inner vestibule play in the slow process of Ba^{2+} exit that resulted from the interaction of K^+ ions in the inner vestibule with the Ba^{2+} bound in the selectivity filter. Furthermore, in the presence of polyamine competition for binding sites, the dose response effect of intracellular potassium ion concentration ($[K^+]_i$) on Ba^{2+} exit was recorded. The results revealed that Ba^{2+} exit to the extracellular side is facilitated by cooperative binding of at least three K^+ ions. Simulations based on sequential binding models could not reproduce the effects of $[K^+]_i$ on Ba^{2+} exit. Because ions not only bind but also move in channels, and because many water molecules separate K^+ and Ba^{2+} ions in the inner vestibule, we propose that in addition to K^+ binding, concerted K^+ transport in the inner vestibule is involved in Ba^{2+} exit. Both a D172N mutation that affects K^+ movement in the water cavity (Bichet et al., 2006) and reduced ion-ion interactions induced by ion mixtures (Hille, 2001) decrease the steepness of the effects of $[K^+]_i$ on Ba^{2+} exit, thus supporting the concerted K^+ transport hypothesis.

(1) Bichet,D., M.Grabe, Y.N.Jan, and L.Y.Jan. 2006. Electrostatic interactions in the channel cavity as an important determinant of potassium channel selectivity. *Proc. Natl. Acad. Sci. U. S. A* 103:14355-14360.

(2) Hille,B. 2001. Selective Permeability: Saturation and Binding. *In* Ionic channels of excitable membranes. Sinauer, Sunderland.

IL09

Right or left turn ? RecA family protein filaments promote homologous recombination through clockwise axial rotation.

Ting-Fang Wang

Institute of Biomedical Science, Academia Sinica, Taipei, Taiwan

Correspondence e-mail address: tfwang@gate.sinica.edu.tw

The RecA family proteins mediate homologous recombination, a ubiquitous mechanism for repairing DNA double-strand breaks ÅDSBsÇ and stalled replication forks. Members of this family include bacterial RecA, archaeal RadA, and eukaryotic proteins Rad51 and Dmc1. These proteins bind to single-stranded DNA at a DSB site to form a presynaptic nucleoprotein filament, align this presynaptic filament with homologous sequences in another double-stranded DNA segment, promote DNA strand exchange and then dissociate. It was generally accepted that RecA family proteins function throughout their catalytic cycles as right-handed helical filaments with six protomers per helical turn. However, we recently reported that archaeal RadA proteins could also form an extended right-handed filament with three monomers per helical turn and a left-handed protein filament with four monomers per helical turn. Additional structural and functional analyses suggest that RecA family protein filaments, similar to the F1-ATPase rotary motor, perform ATP-dependent clockwise axial rotation during their catalytic cycles. This new hypothesis has opened a new avenue for understanding the molecular mechanism of RecA family proteins in homologous recombination.

(1) TF Wang, L Chen and AHJ Wang. (2008) Right or left turn? RecA family protein filaments promote homologous recombination through clockwise axial rotation. *BioEssays* **30,** 4856.

IL10

Microbial Structural Genomics: Important Biological Functions Executed by Interesting Protein Structures

Chao-Yu Yang[a], Wei-Ting Kuo[a], Ko-Hsin Chin[b], Shan-Ho Chou[a,b,*]

[a] *Institute of Biochemistry, National Chung-Hsing University, Taichung, 40227, Taiwan, ROC*

[b] *National Chung Hsing University Biotechnology Center*

National Chung-Hsing University, Taichung, 40227, Taiwan, ROC

Correspondence e-mail address:shchou@nchu.edu.tw

Structural genomics is crucial for understanding the intricate interactions among proteins in a whole organism. We have studied the structural genomics of *Xanthomonas campestris* (*Xcc*), a gram-negative bacterium that is phytopathogenic to cruciferous plants and causes worldwide agricultural loss. *Xcc* is the only bacterium known to lack a cAMP signaling system, and uses a cAMP-receptor protein like protein (CLP) system instead. Currently we are working on its flagellar and SOS structural genomics.

In the flagellar system, we have solved the first crystal structure of a hook-capping protein FlgD. The core structure reveals a novel hybrid comprising a tudor-like domain interdigitated with a fibronectin type III domain. In the crystal, the monomers form an annular pentamer of dimers of pseudo five-fold symmetry, due to the different dimer-dimer interactions incorporated. The resulting asymmetrical star-like decamer complex has a outer dimensions of approximately 110 A x 90 A x 65 A, and a shortest diameter of approximately 20 A in the center. The outer dimensions of the atomic *Xcc* hook-capping FlgD complex turn out to be very similar to those of the *Salmonella* filament cap complex observed by electron microscopy.

SOS has been the most intensively studied system induced under DNA damage, and is characterized by the induction of more than 20 genes, which are under the control of LexA. In response to DNA damage, RecA is activated to induce the auto-cleavage of LexA, resulting in de-repression of genes in the SOS regulon. The recX gene is co-transcribed with recA and its product is suggested to regulate RecA function by directly interacting with RecA protein. We have solved the first RecX structure to a resolution of 1.6 A. It is a curved structure comprising three tandem repeats R1, R2 and R3 of three-helix bundles. Model studies indicate RecX can fit into the helical groove of the RecA filament very well, similar to that reported for the cryoEM image of the RecA/RecX/ATP/ssDNA complex.

IL11

Structure and function of the *E. coli* bifunctional protein glutathionylspermidine synthetase/ amidase

Chien-Hua Pai[1,3], Bing-Yu Chiang[1,4], Tzu-Ping Ko[1], Chia-Cheng Chou[2], Cheong-Meng Chong[1], Fang-Jiun Yen[1], Shunjun Chen[5], James K. Coward[5], Andrew H.-J. Wang[*,1,2,4] and Chun-Hung Lin[#,*,1,2,4]

[1] *Institute of Biological Chemistry, Academia Sinica, Taipei, 11529, Taiwan*

[2] *Genomics Research Center, Academia Sinica, Taipei, 11529, Taiwan*

[3] *Institute of Biochemistry, National Yang-Ming University, Taipei, 11221, Taiwan*

[4] *Institute of Biochemical Sciences, College of Life Science, National Taiwan University, Taipei, 10617, Taiwan*

[5] *Department of Medicinal Chemistry & Chemistry, University of Michigan, Ann Arbor, MI 48109-1055, USA*

Correspondence e-mail address: pai0326@gate.sinica.edu.tw

Most organisms use glutathione to regulate intracellular thiol redox balance and protect against oxidative stress; protozoa, however, utilize trypanothione for this purpose. Trypanothione biosynthesis requires ATP-dependent conjugation of glutathione (GSH) to the two terminal amino groups of spermidine by glutathionylspermidine synthetase (GspS) and trypanothione synthetase (TryS), which are considered as drug targets.GspS catalyzes the penultimate step of the biosynthesis— amide bond formation between spermidine and the glycine carboxylate of glutathione. We report the full length X-ray structures of *Escherichia coli* GspS in complex with C-terminal synthetase substrate, product or inhibitor. The C-terminal of GspS belongs to the ATP grasp superfamily with similar fold to the human glutathione synthetase. Based on our structure we propose that GSH is phosphorylated at one of two GSH binding sites to form an acylphosphate intermediate that then translocates to the other site for subsequent nucleophilic addition of spermidine. We also identify essential amino acids involved in the synthetase catalysis. Our results constitute the first structural information on the biochemical features of parasite homologs (including TryS) that underlie their broad specificity for polyamines.

The amidase activity residues in the N-terminal region of the bifunctional protein and has been proposed to use Cys59 as the catalytic nucleophile. Interestingly the amidase is selectively inactivated when treated with hydrogen peroxide, but the synthetase activity remained mainly intact. We have resolved the amidase structures by X-ray crystallography under various conditions. The results not only elucidate the catalytic mechanism, but also indicate the formation of sulfenic acid upon the addition of hydrogen peroxide. Our current preliminary evidence suggests that the inactivated amidase results in the accumulation of Gsp that has higher reduction potential than GSH, in order to respond the oxidative stress.

IL12

Functional Roles of the Novel 6-*S*-Cysteinyl, 8α-*N1*-Histidyl FAD in Glucooligosaccharide Oxidase from *Acremonium strictum*

Shwu-Huey Liaw

Department of Life Sciences and Institute of Genome Sciences, National Yang-Ming University, Taipei, Taiwan

Correspondence e-mail address: shliaw@ym.edu.tw

Recently, we have determined crystal structures of glucooligosaccharide oxidase (GOOX) from *Acremonium strictum*, which unexpectedly demonstrate the first known double attachment flavinylation to His 70 and Cys130, 6-*S*-cysteinyl, 8α-*N1*-histidyl FAD. The H70A and C130A single mutants still retain the covalent FAD, indicating that flavinylation at these two residues is independent. The wild-type and the H70A and C130A mutant proteins exhibit a midpoint potential of +126, +70 and +61 mV, respectively. The single mutants still possess residual activity, but the k_{cat} values reduced to about 2% and 5%, while the flavin reduction rate to 0.6% and 14%, compared to the wild-type GOOX. These indicate that both covalent linkages alter the redox properties of the FAD cofactor leading to decreased catalytic efficiency of the mutants. In addition, the crystal structure of the C130A mutant displays conformational changes not only in the isoalloxazine ring but also in several residues surrounding Cys130. The latter includes two substrate-interacting residues, Thr129 and Tyr300, consistent with the increased *Km* value. Then the C130A structure provides direct evidence for a novel function of 6-*S*-cysteinylation in assistance of substrate binding. Furthermore, the isolated H70A/C130A double mutant does not contain FAD, and addition of exogenous FAD was not able to restore any detectable activity, suggesting that the cofactor binding precedes the covalent attachment and the covalent bond ensures saturation of the active site with the cofactor. Finally, the wild-type enzyme is more heat and guanidine-HCl resistant than any of the mutants investigated in this study. Therefore, the bicovalent flavin linkage enhances not only the cofactor binding, the redox potential, the substrate binding but also the stability of the protein structure. The characteristics of the covalent FAD/FMN in other related flavoenzymes will be also compared.

(1) Huang et al. (2005) *J. Biol. Chem.* **280**, 38831-38838

(2) Huang et al. (2008) manuscript in submission

IL13

NMR Structure and Backbone Dynamics of Streptopain: Insight into Diverse Substrate Specificity

Woei-Jer Chuang, Chih-Chieh Wang, Hsiang-Chee Houng, and Chun-Liang Chen

Departments of Biochemistry and Molecular Biology, National Cheng Kung University College of Medicine, Tainan, Taiwan

Correspondence e-mail address: wjcnmr@mail.ncku.edu.tw

Streptococcal pyrogenic exotoxin B (SPE B) is a cysteine protease expressed by Streptococcus pyogenes. In order to study the effect of the allelic polymorphism on the protease activity of SPE B, the D9N, G163S, G163S/A172S, and G239D mutant proteins have been expressed in E. coli and purified to homogeneity. The activities of D9N, G163S, and G163S/A172S mutants were 1-2 folds less than that of wild-type protein. Interestingly, the G239D mutant was ~12-fold less active. However, the G239 residue is located in the C-terminal loop (R223-Q245), and the S230-G240 region cannot be observed in X-ray structure. To understand the role of the C-terminal loop, we used NMR spectroscopy to determine 3D structures and backbone dynamics of 28-kDa mature SPE B and its inhibitor complexes. Unlike X-ray structure of 40-kDa zymogen SPE B, we observed interactions between the residues in the catalytic loop (V47 and A196) and the residues in the C-terminal loop (A231 and A238) of 28-kDa mature SPE B. The catalytic loop (G188-F197) and the X-ray unobservable region (S230-G240) of 28-kDa mature NMR structure were found to be close to each other. Dynamics analysis of SPEB and the SPE B/inhibitor complexes showed that the catalytic and C-terminal loops were the most flexible regions with low order parameter values of 0.5-0.7 and exhibited the motion on the ps/ns timescale. These findings suggest that the flexible C-terminal and catalytic loops of SPE B many play an important role in controlling the substrate binding, resulting in its broad substrate specificity.

(1) Chen, C.-Y., Luo, S.-C., Kuo, C.-F., Lin, T.-S., Wu, J.-J., Lin. M.-T., Liu, C.-C., Jeng, W.-Y., and Chuang, W.-J. (2003) “Maturation and Characterization of Streptopain”, J. Biol. Chem., 278, 17336-17343.

(2) Wang, C.-C., Chen, C.-L., Houng, H.-C., Kuo, C.-F., Lin, Y.-S., Wu, J.-J., Lin. M.-T., Liu, C.-C., Chen, C.-Y., Huang, W., and Chuang, W.-J. (2008) “Solution Structure and Backbone Dynamics of Streptopain: Insight into Diverse Substrate Specificity”, submitted.

IL14

Dissecting the Structure and Nucleic Acid Packaging Mechanism of SARS Coronavirus Nucleocapsid Protein

Tai-huang Huang

Institute of Biomedical Sciences, Academia Sinica, Taipei, Taiwan

Department of Physics, National Taiwan Normal University, Taipei, Taiwan

Correspondence e-mail address: *bmthh@ibms.sinica.edu.tw*

Coronavirus nucleocapsid proteins encapsulate viral genomic RNA to form part of the virus structure. The nucleocapsid protein of SARS-CoV is highly antigenic and associated with several host-cell interactions. Using NMR we showed that NP consists of two structured domain, a N-terimnal domain (NTD, a.a. 45-181) and a C-terminal domain (CTD, a.a. 248-365), franked by three long disordered regions. We further showed that the CTD forms dimer and it is capable of binding to RNA. The structure of CTD was further solved by both NMR and X-ray crystallography. To overcome the size problem the solution structure of the 28 kDa dimer was solved by stereo-array isotope labeling (SAIL) method utilizing a protein exclusively composed of stereo- and regio-specifically isotope labeled amino acids. Packing of the CTD octamers in an asymmetric unit cell of the crystal forms two parallel, basic helical grooves which is presumed to be the oligonucleotide attachment sites, and suggests a mechanism for helical RNA packaging in the virus. Studies of the NMR chemical shift perturbations caused by the binding of single-stranded DNA and mutational analyses have identified the disordered region at the N-termini as the prime site for nucleic acid binding. In addition, residues in the β-sheet region also showed significant perturbations. Mapping of the locations of these residues onto the helical model observed in the crystal revealed that these two regions are parts of the interior lining of the positively charged helical groove, supporting the hypothesis that the helical oligomer may form in solution. Systematic mapping of possible nucleic acid binding sites on the full length protein identified multiple potential nucleic acid binding sites, suggesting a multiple RNA binding initiation sites and a model of packaging is proposed.

(1) Hsieh, P.K. et al (2005) “The Assembly of an RNA Packaging Signal Containing Virus-Like Particle of SARS-CoV is Nucleocapsid-dependent” J. Virol. **79,** 13848-13855.

(2) Chang, C.K.et al (2005) “The dimer interface of the SARS coronavirus nucleocapsid protein adapts a porcine respiratory and reproductive syndrome virus-like structure” FEBS Lett. **579**, 5663-5668.

(3) Chang, C.K. et al. (2006) “Modular organization of SARS coronavirus nucleocapsid protein”. J. Biomed. Sci. 13, 59-72.

(4) Chen, C.Y. et al. (2007) “Structural insights into packaging of the helical nucleocapsid from the crystal structure of SARS coronavirus nucleocapsid protein dimerization domain”, J. Mol. Biol. 368, 1075-1086.

(5) Takeda, M.et al. (2008) “Solution Structure of the C-terminal Dimerization Domain of SARS Coronavirus Nucleocapsid Protein Solved by the SAIL-NMR Method” J. Mol. Biol. (in press).

IL15

Novel Physical Biotechnology Development and Its Applications

Chung Hsuan (Winston) Chen

Genomics Research Center, Academia Sinica, Taipei, Taiwan

Recently, we have developed a few novel physical biotechnologies which includes (1) Laser desorption mass spectrometry for rapid proteomic analysis (2) Novel cell mass spectrometry and (3) Nanoparticle-labeled microarray. The purpose, approach and results of each technology will be presented. Future perspective will also be discussed.

IL16

Mining Phosphopeptide Signals in Liquid Chromatography-Mass Spectrometry Data for Protein Phosphorylation Analysis

Pao-Chi Liao

Department of Environmental and Occupational Health, College of Medicine,

National Cheng Kung University, Tanani, Taiwan

Correspondence e-mail address: liaopc@mail.ncku.edu.tw

Protein phosphorylation is a key post-translational modification that governs biological processes. Despite a number of analytical strategies have been exploited for the characterization of protein phosphorylation, the identification of protein phosphorylation sites is still challenging. We proposed here an alternative approach to mine phosphopeptide signals generated from a mixture of proteins when liquid chromatography-tandem mass spectrometry (LC-MS/MS) analysis is involved. The approach combined dephosphorylation reaction, accurate mass measurements from a quadrupole/time-of-flight mass spectrometer, and a computing algorithm to differentiate possible phosphopeptide signals obtained from the LC-MS analyses by taking advantage of the mass shift generated by alkaline phosphatase treatment. The retention times and m/z values of these selected LC-MS signals were used to facilitate subsequent LC-MS/MS experiments for phosphorylation site determination. Unlike commonly used neutral loss scan experiments for phosphopeptide detection, this strategy may not bias against tyrosine-phosphorylated peptides. We have demonstrated the applicability of this strategy to sequence more, in comparison with conventional data-dependent LC-MS/MS experiments, number of phosphopeptides in a mixture of α- and β-caseins. The analytical scheme was applied to characterize the nasopharyngeal carcinoma (NPC) cellular phosphoproteome and yielded 221 distinct phosphorylation sites. Our data presented in this report demonstrated the merits of computation in mining phosphopeptide signals from a complex mass spectrometric dataset.

IL17

A D-form Pro mutant of Aβ40 forms a new amyloid–like β-aggregate and is able to attenuate the cytotoxicity of Aβ40

Rita P.-Y. Chen

Institute of Biological Chemistry, Academia Sinica, Taipei, Taiwan

Correspondence e-mail address: pyc@gate.sinica.edu.tw

The residue immediately preceding each glycine in the 40 amino acid Aβ40 peptide (S8, V24, I32, and V36) was individually replaced by D-form proline (^{D}Pro). The resulting ^{D}P-G sequence (the ^{D}Pro residue and the following Gly residue) was designed as a “structural clip” to force the formation of a bend in the peptide, as this sequence has been reported to be a strong promoter of β-hairpin formation. The mutated peptides (V24, I32, and V36) no longer formed an amyloid fibril structure, although they still went through a coil-to-β structural conversion. At a low peptide concentration, a random coil structure was formed, while, at a high peptide concentration, a non-fibril β-sheet structure was formed. The converted β-structure is not as stable as the amyloid fibrils formed from the wild-type Aβ40 peptide and can be converted back by simple dilution. Interestingly, Thioflavin T and Congo red, the dyes usually employed in amyloid detection and quantification, were able to bind to thiș β-sheet structure. We concluded that these Aβ mutants form a new amyloid-like aggregate. Moreover, the mutant peptide V24P, when mixed with Aβ40, can attenuate the cytotoxicity of Aβ40.

IL18

Ion interaction and free radical generation of β-amyloid peptides

Yi-Cheng Chen

Institute of Biomedical Technology, Tzu Chi University, Hualien, Taiwan

The aggregation and deposition of β-amyloid (Aβ) is the main cause of Alzheimer's disease. The Aβ aggregates have been proposed to generate free radicals in the presence or absence of Cu^{2+}. In a previous study of our group (J. Biochem., 2006, 139, 73-740), the structure of monomeric Aβ can be characterized into three structural states, including random coil, unstable helix, and stable helix. Therefore, we applied these structural states of Aβ and re-examined whether free radicals can be generated at these states. Unlike the usual hypothesis that only aggregated Aβ can produce free radicals, our results demonstrate that even monomeric Aβ can produce free radicals in the presence of Cu^{2+}, and the generation of free radical is dependent on the structure of monomeric Aβ and the affinity of Cu^{2+}. Only monomeric Aβ in the stable helix state could also induce the free radical generation in the presence of Cu^{2+}, while monomeric Aβ in random coil and unstable helix states showed to inhibit the free radical generation within a short time scale. This structure-dependent free radical generation may be further associated with the interaction of Cu^{2+}. As result shown, the copper affinity is also structure-dependent. The weaker copper-affinity, the stronger free radical generation.

IL19

Force-induced oscillations of polymerizing actin gels

Hsuan-Yi Chen[1,2] , Jean-Francois Joanny[3], and Jacques Prost[3,4]

[1]*Department of Physics and Institute of Biophysics, National Central University, Jhongli, Taiwan*

[2]*Institute of Physics, Academia Sinica, Taipei, Taiwan*

[3]*Physicochimie Curie (CNRS-UMR168), Institut Curie, Section de Recherche*

26 rue d'Ulm, 75248 Paris Cedex 05, France

[4]*ESPCI - 10 rue Vauquelin, 75231 Paris Cedex 05, France*

Correspondence e-mail address:hschen@phy.ncu.edu.tw

Actin filaments are polar filaments with ATP-actin monomers on its barbed end and ADP-actin monomers on its pointed end. In solution there exists a steady state in which the barbed end grows and the pointed end shrinks, this is called treadmilling. Treadmilling is thought to be responsible for the steady movement of the lamellipodia during cell motility. Under external force the ratio between the polymerization rate and the depolymerization rate of the barbed end decreases due to the energy cost for adding a new monomer to the barbed end. As a result the moving velocity of a motile cell decreases as the drag force on the cell increases monotonically. However, a recent experiment has shown that strong nonlinear effects could change this simple physical picture and it could be common for growing actin network to oscillate cooperatively under external force. A phenomenological theory that models this experiment is presented. Our model includes nonlinear elastic properties of actin network and non-monotonic relation between external force and polymerization rate. We find that under certain conditions the steady "stall" configuration loses stability, and the system undergoes a Hopf bifurcation so that the actin gel starts to oscillate. The biological implication of our analysis and possible future experiments and theoretical works are discussed.

IL20

Local Hydrophobicity and Protein Secondary Structure Formation

Ming-Chya Wu[1,2]

[1]*Research Center for Adaptive Data Analysis, National Central University, Chungli 32001, Taiwan*

[2]*Institute of Physics, Academia Sinica, Taipei 11529, Taiwan*

Correspondence e-mail address: mcwu@ncu.edu.tw

The local hydrophobicity (LHP) around a residue defined as the sum of hydrophobicity (HP) values of residues surrounding the residue within a specified distance was calculated based on the structure of staphylococcal nuclease (SNase) in the Protein Data Bank. According to the geometrical constraint of native protein structures [1] and the experimental evidence that the dimension of the denatured states of SNase is compact [2], we assumed the three-stages folding model [3] to investigate the effects of LHP in the folding of SNase. Based on the correlation between HP and LHP, we formulated the correlation coefficient between LHP and secondary structure at each residue to estimate the percentage contents of secondary structures from changes of LHPs in mutants. The estimations are qualitatively and quantitatively consistent with those from Circular Dichroism measurements on mutants W140A (Tryptophan at 140 is replaced by Alanine), F61W/W140A, Y93W/W140A and E75G [4].

(1) M.-C. Wu, M. S. Li, M. Kouza, W.-J. Ma, and C.-K. Hu, Geometrical constraint on native protein structures, manuscript submitted (2008).

(2) C.-Y. Chow, M.-C. Wu, H.-J. Fang, C.-K. Hu, H.-M. Chen, and T.-Y. Tsong, Compact dimension of denatured states of staphylococcal nuclease, Proteins: Struct. Func. Bioinfo., in press (2008).

(3) T.-Y. Tsong, C.-K. Hu, and M.-C. Wu, Hydrophobic condensation and modular assembly model of protein folding, Biosystems, in press (2008).

(4) M.-C. Wu, C.-K. Hu, H.-M. Chen, and T.-Y. Tsong, Local hydrophobicity and protein secondary structure formation: Theoretical model and experimental test, manuscript submitted (2008).

IL21

Scalings Properties in the Aggregation of Slime Mould

W. Chen[1], S. F. Hsu[1], P. Y. Lai[2], and C.K. Chan[1,2]

[1]*Institute of Physics, Academia Sinica, Taipei, Taiwan*

[2]*Graduate Institute of Biophysics, National Central University, Chungli, Taiwan*

Correspondence e-mail address: ckchan@gate.sinica.edu.tw

Aggregation of slime mould on top of an agar plate is studied with video microscopy as a function of cell plating densities (ρ). We find that the aggregation can be described by the parameter $\varepsilon = (\rho - \rho_\chi)/\rho$ with ρ_c being the critical density below which no slugs can be formed. Our experimental results show that the aggregation time (T) scales as: $T \sim \varepsilon^{-a}$ while the size V of the aggregate as: $V \sim \log(\varepsilon)$. It is found that some aspect of these scaling behaviors can be understood by a density dependent persistent time (τ) which describes well the motions of pre-aggregative cells by a persistent random walk as: $\langle r^2(t) \rangle = 4D(t - \tau(1-e^{-t/\tau}))$ with r being the displacement and D the motility of the cells. Implications of these findings will be discussed.

IL22

Inverse symmetry in genomes and whole-genome inverse duplication

Sing-Guan Kong[1], Wen-Lang Fan[1], Hong-Da Chen[1], HC Lee[1,2]

[1]*Department of Physics, National Central University, Taiwan*

[2]*Graduate Institute of Systems Biology and Bioinformatics, National Central University, Taiwan*

Correspondence e-mail address: hclee@phy.ncu.edu.tw

Segmental duplication has long been known to be an important mechanism for genome growth and evolution (Lynch 2002, Bailey et al. 2002), and recently it has been firmly established that whole-genome duplications have at least occurred in yeast (Wolfe and Shields 1997) and in some species of fishes ray-finned fishes. Here we present evidence showing that whole-genome inverse duplication very likely occurred in one half of eubacterial genomes, and possibly in most chromosomes, prokaryotic as well as eukaryotic. We derive our evidence through a comprehensive study of the inverse symmetry in all publicly available complete genomes. We find that a vast majority of chromosomes have close to maximum global inverse symmetry, but the chromosomes exhibit starkly distinct patterns of local inverse symmetry. These patterns provide clues for a consistent narrative of the many ways inverse segmental duplications may have occurred in genomes.

Segmental duplication has long been known to be an important mechanism for genome growth and evolution (Lynch 2002, Bailey et al. 2002), and recently it has been firmly established that whole-genome duplications have at least occurred in yeast (Wolfe and Shields 1997, Wapinski et al. 2007) and in some species of fishes ray-finned fishes. Here we present evidence showing that whole-genome inverse duplication very likely occurred in one half of eubacterial genomes, and possibly in most chromosomes, prokaryotic as well as eukaryotic. We derive our evidence through a comprehensive study of the inverse symmetry in all publicly available complete genomes. We find that a vast majority of chromosomes have close to maximum global inverse symmetry, but the chromosomes exhibit starkly distinct patterns of local inverse symmetry. These patterns provide clues for a consistent narrative of the many ways inverse segmental duplications may have occurred in genomes.

(1) Lynch, M. 2002. Genomics. Gene duplication and evolution. *Science* 297: 945-947.

(2) Bailey, J.A., Z. Gu, R.A. Clark et al. 2002. Recent segmental duplications in the human genome. *Science* 297: 1003-1007.

(3) Wolfe, K.H. and D.C. Shields. 1997. Molecular evidence for an ancient duplication of the entire yeast genome. *Nature* 387: 708-713.

(4) Wapinski, I., A. Pfeffer, N. Friedman, and A. Regev. 2007. Natural history and evolutionary principlesof gene duplication in fungi. *Nature* 449: 54-61.

IL23

An Intelligent Two-Stage Evolutionary Algorithm for Dynamic Pathway Identification from Gene Expression Profiles

Shinn-Ying Ho[1,2], Chih-Hung Hsieh[2], Fu-Chieh Yu[2] and Hui-Ling Huang[3]

[1]*Department of Biological Science and Technology, National Chiao Tung University, Hsinchu, Taiwan*

[2]*Institute of Bioinformatics, National Chiao Tung University, Hsinchu, Taiwan*

[3]*Department of Information Management, Jin Wen Institute of Technology, Taipei, Taiwan*

Correspondence e-mail address: syho@mail.nctu.edu.tw

From gene expression profiles, it is desirable to rebuild cellular dynamic regulation networks to discover more delicate and substantial functions in molecular biology, biochemistry, bioengineering, and pharmaceutics. The S-system model is suitable to characterize biochemical network systems and capable of analyzing the regulatory system dynamics. However, the inference of an S-system model of N-gene genetic networks has 2N(N+1) parameters in a set of non-linear differential equations to be optimized. This paper proposes an intelligent two-stage evolutionary algorithm (iTEA) to efficiently infer the S-system models of genetic networks from time-series data of gene expression. To cope with curse of dimensionality, the proposed algorithm consists of two stages where each uses a divide-and-conquer strategy. The optimization problem is first decomposed into N subproblems having 2(N+1) parameters each. At the first stage, each subproblem is solved using a novel intelligent genetic algorithm (IGA) with intelligent crossover based on orthogonal experimental design (OED). At the second stage, the obtained N solutions to the N subproblems are combined and refined using an OED-based simulated annealing algorithm for handling noisy gene expression profiles. The effectiveness of iTEA is evaluated using simulated expression patterns with and without noise running on a single-processor PC. It is shown that 1) IGA is efficient enough to solve subproblems, 2) IGA is significantly superior to the existing method SPXGA, and 3) iTEA performs well in inferring S-system models for dynamic pathway identification.

(1) S.-Y. Ho*, C.-H. Hsieh, F.-C. Yu and H.-L. Huang, “An intelligent two-stage evolutionary algorithm for dynamic pathway identification from gene expression profiles,” *IEEE/ACM Trans. Computational Biology and Bioinformatics*, pp. 648-660, 2007.

IL24

Regulatory mechanisms of adjacent genes in yeast

Huai-Kuang Tsai

Institute of Information Science, Academia Sinica, Taipei, Taiwan

Correspondence e-mail address: hktsai@iis.sinica.edu.tw

Adjacent gene pairs in the yeast genome have a tendency to express concurrently. Sharing of regulatory elements within the intergenic region of those adjacent gene pairs was often considered the major mechanism responsible for such co-expression. However, it is still in debate to what extent that common transcription factors (TFs) contribute to the co-expression of adjacent genes. In order to resolve the evolutionary aspect of this issue, we investigated the conservation of adjacent pairs in five yeast species. By using the information for TF binding sites in promoter regions available from the MYBS database http://cg1.iis.sinica.edu.tw/~mybs/, the ratios of TF-sharing pairs among all the adjacent pairs in yeast genomes were analyzed. The levels of coexpression in different adjacent patterns were also compared.

Our analyses showed that the proportion of adjacent pairs conserved in five yeast species is relatively low compared to that in the mammalian lineage. The proportion was also low for adjacent gene pairs with shared TFs. Particularly, the statistical analysis suggested that coexpression of adjacent gene pairs was not noticeably associated with the sharing of TFs in these pairs. We further proposed a case of the PAC (polymerase A and C) and RRPE (rRNA processing element) motifs which co-regulate divergent/bidirectional pairs, and found that the shared TFs were not significantly relevant to co-expression of divergent promoters among adjacent genes.

Our findings suggested that the commonly shared *cis*-regulatory system does not solely contribute to the co-expression of adjacent gene pairs in yeast genome. Therefore we believe that during evolution yeasts have developed a sophisticated regulatory system that integrates both TF-based and non-TF based mechanisms(s) for concurrent regulation of neighboring genes in response to various environmental changes.

IL25

Protein modification analyses using Fourier transformation Orbitrap mass spectrometry

Yeou-Guang Tsay[1,2], Nai-Yu Liu[1], and Cheng-Hung Chao[1]

[1]*Instiute of Biochemistry & Molecular Biology, National Yang-Ming University, Taipei, Taiwan*

[2]*Proteomics Research Center, National Yang-Ming University, Taipei, Taiwan*

Correspondence e-mail address: ygtsay@ym.edu.tw

Mapping of modified residues in proteins has been a major challenge in biomedical research. Although major progress has been made in large-scale identification of phosphopeptides, the vast majority of protein modifications remain uncharacterized. We have developed a comprehensive modification mapping procedure that can survey a multitude of protein modifications in a single analysis. In order to detect the modified peptides of lower abundance, we first optimized the data collection method to increase the dynamic range of Orbitrap mass spectrometer. We then devised a collection of macro programs to facilitate the identification of protein modifications using these mass spectrometric data. This method is particularly suitable for the analyses of clinical specimens like human plasma. Up to date, we have uncovered many novel protein modifications in plasma proteome from normal individuals, including *O*-linked glycosylation, phosphorylation, hydroxylation, carboxylation and glycation. Mass spectrometric methods will be developed to speed up the quantitative analyses of these protein modifications. We hope that protein modifications associated with specific human diseases can thus be identified.

IL26

Protein Acetyltransferases and Related Chromatin Proteins *in* *Sulfolobus solfataricus* P2: Structural and Chemical Proteomics Approaches

Chun-Hua Hsu

Institute and Department of Agricultural Chemistry, National Taiwan University, Taipei, Taiwan

Correspondence e-mail address: andyhsu@ntu.edu.tw

Organisms growing at elevated temperatures face the challenge of maintaining the integrity of their genetic materials. Archaea possess unique chromatin proteins but not histones for gene organization and information processing. Several small DNA-binding proteins, such as Alba (acetylation lowers binding affinity) (1), Sso7c4 (2) and Sso7d (3) from hyperthermophilic organism *Sulfolobus solfataricus* P2 were found and have been proposed to play a regulatory role in gene transcription and chromatin formation; however, very little is known regarding the structural and functional relationship as well as the covalent modification (like the “histone code”) of these proteins.

Recently, a *Sulfolobus* homolog of the conserved Sir2 NAD-dependent deacetylase was found to interact and deactylate with Alba (4). The chromatin protein should be regulated by reversible acetylation. The potential protein acetyltransferases in *Sulfolobus solfataricus* P2 were identified using bioinformatics search and the selected targets were cloned, expressed and purified. The activities of acetyltransferases were determined by biochemical methods and the acetylated site of chromatin proteins are tried to be identified using mass spectroscopy. The chemical proteomics approach for the new substrates of acetyltransferases is developing and in progress. In addition, structural sub-proteomics of the acetyltransferases and the chromatin proteins are carried out using both multi-dimensional Nuclear Magnetic Resonance (NMR) technique and X-ray diffraction methods.

(1) Wardleworth BN, Russell RJ, Bell SD, Taylor GL, and White MF. Structure of Alba: an archaeal chromatin protein modulated by acetylation. EMBO J. 2002 Sep 2;21(17):4654-62.

(2) Hsu CH, and Wang AH. unpublished data.

(3) Gao YG, Su SY, Robinson H, Padmanabhan S, Lim L, McCrary BS, Edmondson SP, Shriver JW, and Wang AH. The crystal structure of the hyperthermophile chromosomal protein Sso7d bound to DNA. Nat Struct Biol. 1998 Sep;5(9):782-6.

(4) Bell SD, Botting CH, Wardleworth BN, Jackson SP, and White MF. The interaction of Alba, a conserved archaeal chromatin protein, with Sir2 and its regulation by acetylation. Science. 2002 Apr 5;296(5565):148-51.